SHORT REPORT

Figures and figure supplements

Monoallelic *CRMP1* gene variants cause neurodevelopmental disorder

Ethiraj Ravindran, Nobuto Arashiki and Lena-Luise Becker *et al*.

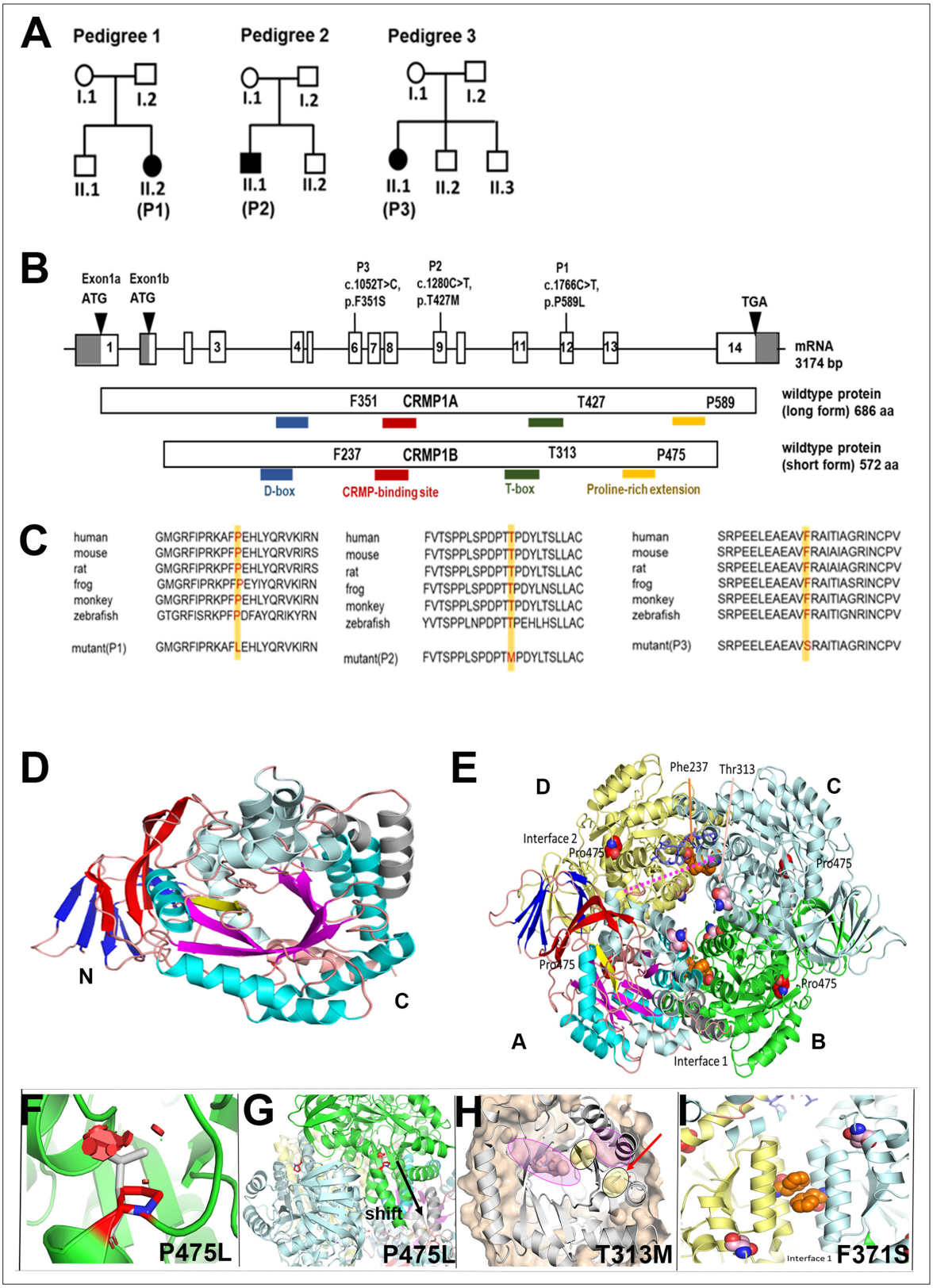

Figure 1. Genotype of patients with variants in *CRMP1*. (**A**) Pedigree of index families. (**B**) Pictogram representing the CRMP1 cDNA with identified variant of proband 1 (P1) in exon 12 (c.1766C>T, NM_001014809.2) which leads on protein level to an amino acid change of proline to leucine in CRMP1 (CRMP1A-long form (p.P589L, NP_001014809.1) and CRMP1B-short form (p.P475L, NP_001304.1)); the variant in proband 2 (P2) in exon 9 c.280C>T (NM_001014809.2) leads to an exchange of threonine to methionine (CRMP1A (p.T427M, NP_001014809.1) and CRMP1B (p.T313M, NP_001304.1)); the

Figure 1 continued on next page

Figure 1 continued

variant in proband 3 (P3) in exon 6 c.052T>C (NM_001014809.2) leads to an exchange of phenyl alanine to serine (CRMP1A (p.(F351S), NP_001014809.1) and CRMP1B (p.(F237S), NP_001304.1)). (**C**) Multispecies sequence alignment localizes the variants in the highly conserved area of CRMP1. (**D**) The short form CRMP1 monomer is composed of three structural parts, an N-terminally located seven β-strands forming two β-sheets (depicted in blue), followed by a linker β-strand (yellow) connecting to the central α/β-barrel (cyan/magenta) formed by seven repeats. Inserted after repeat 4 are 2 additional α-helices (gray). (**E**) CRMP1 assembles into tetramers. The relevant sites of T313M, P475L, and F237S are indicated as sphere model, with the T313 and F237 located in the central channel in the vicinity of the interaction sites and P475 is located at the beginning of the C-terminal helix and oriented toward the adjacent molecules. (**F**) The variant P475L reveals serious clashes with neighboring residues (red hexagonals) which may be accounted for by a shift of the helix as shown in (**G**). (**H**) Detailed representation of the structural vicinity of the T313M (yellow) to the ligand-binding cavity (magenta). (**I**) Magnified view of interface 1 tilted 90° backwards with respect to panel E highlighting the arrangement of the two phenylalanines at position 237 from the neighboring units. The exchange of phenylalanine with hydrophobic residues to serine with hydrophilic side chain interferes with the stability of the interaction in interface 1.

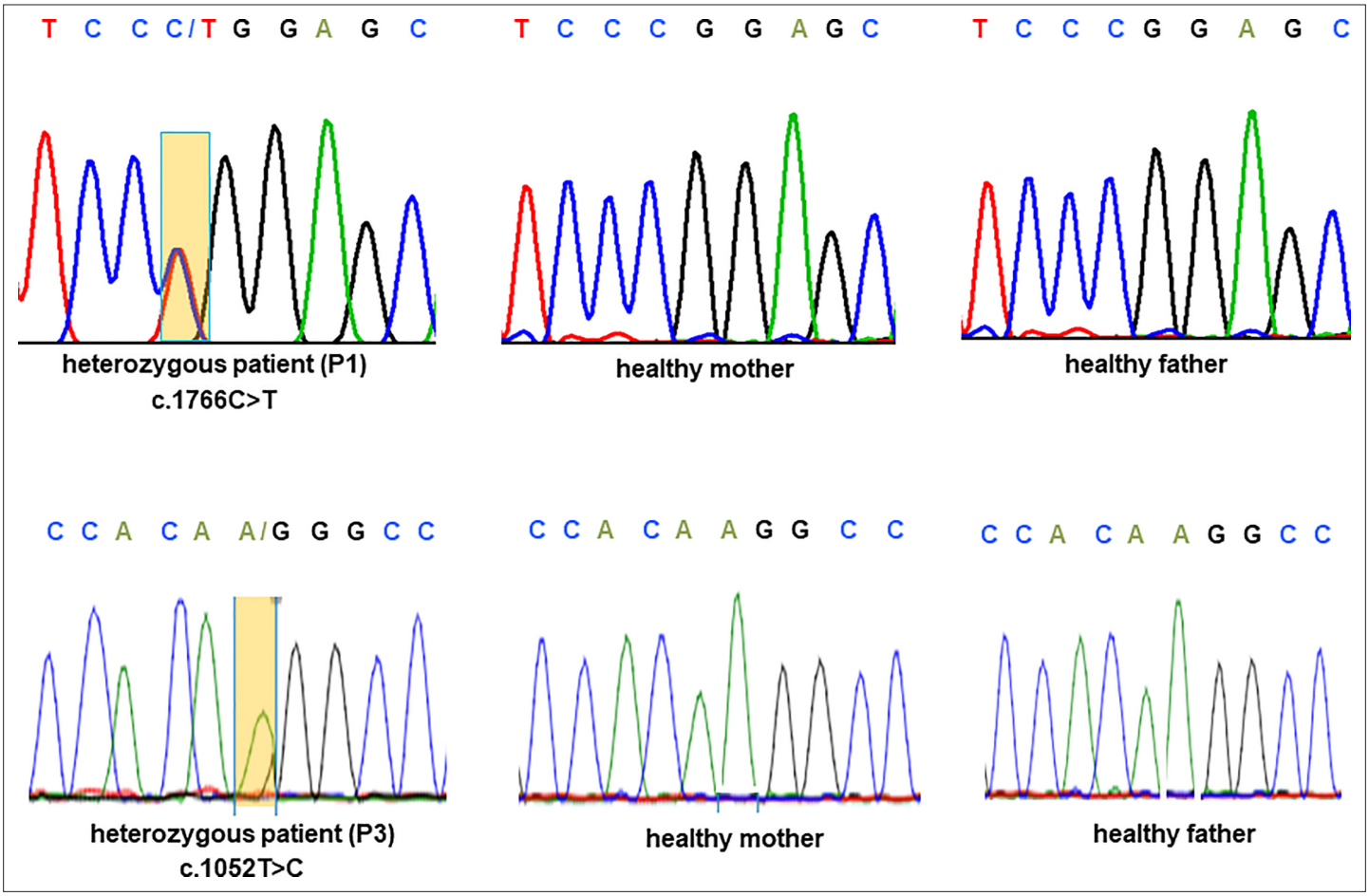

Figure 1—figure supplement 1. Sanger sequencing of *CRMP1* in pedigrees 1 and 3. Electropherogram traces depicting the de novo exchange of c.1766C>T (upper panel) in the proband of pedigree 1 and c.1052T>C (lower panel) in the proband of pedigree 3.

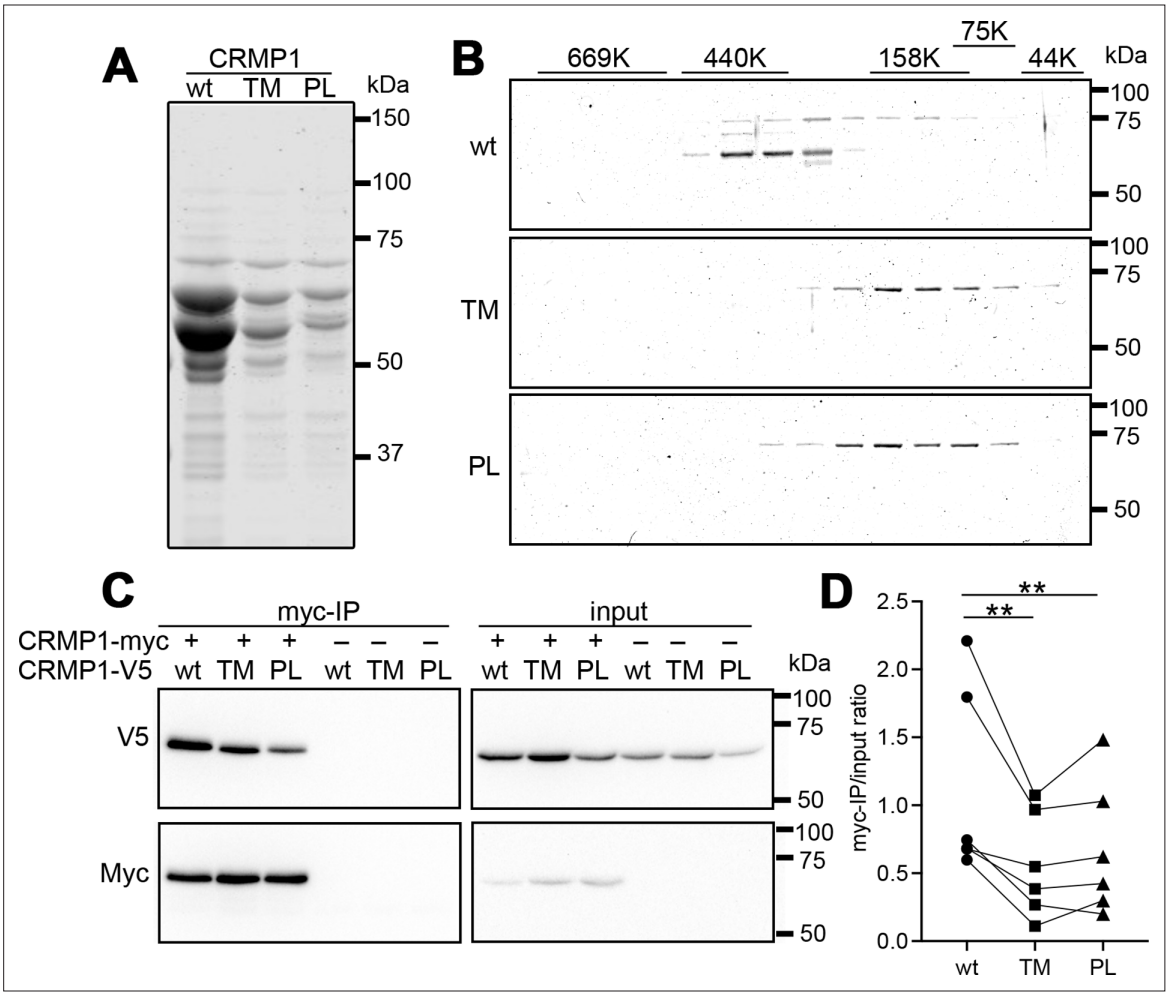

Figure 2. Attenuated oligomer formation of CRMP1-P475L and CRMP1B-T313M variants. (**A**) Purified CRMP1B-wildtype, -T313M, and -P475L recombinant proteins on sodium dodecyl sulfate–polyacrylamide gel electrophoresis (SDS–PAGE) stained with CBB. GST-tagged CRMP1 were expressed in *E. coli* and purified through the binding to glutathione resin and the digestion with PreScission protease. Equal volume (2.5 µl) of the purified specimens, which were prepared under the same condition, were loaded on the gel. The yield of the variants was less than that of CRMP1-wildtype as shown in panel. Two major 64 and 60 kDa bands in the preparations are full-length and a truncated form, respectively. (**B**) Fractionation of CRMP1B specimens by size-exclusion chromatography. Purified CRMP1B specimens (150 µg) were passed through a Sephacryl S-300 column and the resultant flows/elution volumes were fractionated at every 1 ml. SDS–PAGE for 40–86th fractions were carried out after 20 times concentration. The distribution of molecular weights of standard proteins (44–660 kDa) at the same condition was displayed on the top of the gels. (**C**) Reduced homophylic interaction of CRMP1B variants. HEK293T cells coexpressing Myc-tagged CRMP1B-wildtype and either one of V5-tagged CRMP1B-wildtype, -T313M, or -P475L were analyzed by co-immunoprecipitation with anti-Myc-antibody. Immunoprecipitated specimens and input lysates were subjected to anti-V5 and anti-Myc immunoblot analyses. Co-immunoprecipitation of V5-tagged CRMP1 variants were reduced comparing to of wildtype CRMP1-V5. (**D**) Quantification of the V5-signal of Myc-immunoprecipitated specimens and of input lysate. The V5-signal ratios of CRMP1B-T313M and CRMP1B-P475L were significantly decreased compared to the ratio of CRMP1B-wildtype. The graph represents V5-signal ratio of each condition from six independent experiments (n=6). Data were analyzed by one-way repeated measures analysis of variance (ANOVA) followed by Tukey's multiple comparisons test. **p < 0.01. Abbreviations: CRMP1B-wildtype, wt; CRMP1B-T313M, TM; CRMP1B-P475L, PL.

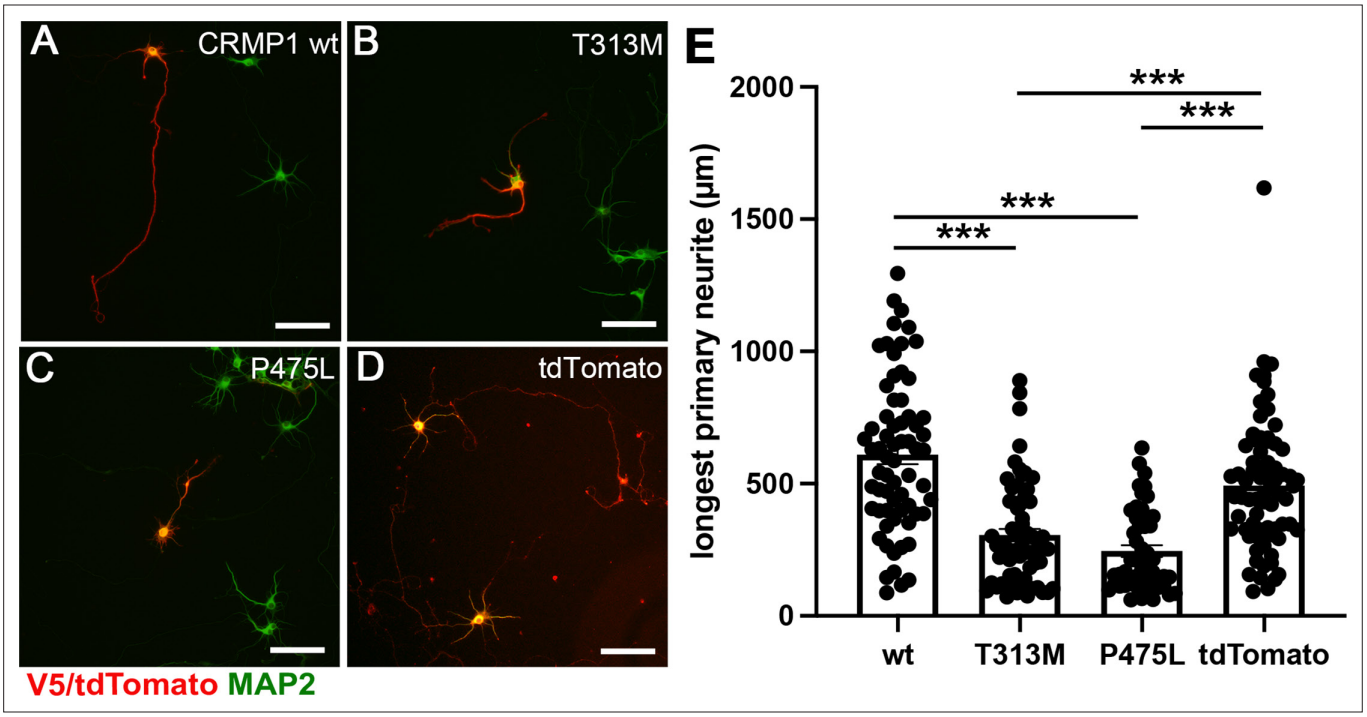

Figure 3. Attenuated neurite outgrowth by the ectopic expression of CRMP1B- P475L and CRMP1B-T313M variants. Representative images of the neurons expressing V5-CRMP1B-wildtype (**A**), -T313M (**B**), -P475L (**C**), or tdTomato (**D**). Transfected neurons were visualized by anti-V5 immunostaining or tdTomato expression (red) and anti-MAP2 immunostaining (green). The longest primary neurites of the neurons expressing V5-CRMP1B-T313M or -P475L were shorter than those of the neurons transfected with V5-CRMP1B-wildtype or tdTomato. Scale bars, 100 μm. (**E**) Longest primary neurite length. The length of the longest primary neurite from V5- or tdTomato-positive neurons was scored in each condition. The graph represents average ± standard error of the mean (SEM) with individual values from four independent experiments. The number (n) of examined neurons in each condition: CRMP1B-wildtype, 66; -T313M, 64; -P475L, 49; tdTomato, 73. Data were analyzed by one-way analysis of variance (ANOVA) followed by Tukey's post hoc test. ***$p < 0.001$.